Effect of saline sedimentary environment on pore throats of shale

Z. X. Zhao[1]*, S. B. Wu[2], M. W. He[3] and Y. J. Fan[4]

[1]School of Geosciences, Yangtze University, Wuhan, Hubei, China, [2]Research Institute of Exploration and Development, Sinopec Shengli Oilfield Company, Dongying, Shandong, China, [3]CNOOC Research Institute Ltd., Beijing, China, [4]CNPC Xibu Drilling Engineering Company Limited, Urumchi, China

Shale pore throat is one of the key factors affecting shale oil and gas exploitation. In order to study the effect of saline on shale pore throat in the continental lacustrine basin, the paleo-salinity of the lacustrine basin was analyzed using the Couth and Sr/Ba methods, and the pore throat characteristics of shale were observed by thin section and scanning electron microscope. The saline stage is divided into five stages: freshwater (0.5‰−1‰), brackish water (1‰−5‰), brackish water (5‰−15‰), brackish water (15‰−30‰), and high saltwater (>30‰). Shale is mainly reserved in micropores (organic, intercrystalline, and intergranular pores) and microcracks (along-layer, high pressure, structural, and mineral shrinkage cracks). Paleosalinity affects the pore throat characteristics of shale by controlling the mineral composition, rock combination type, and texture. Carbonate minerals tend to dissolve and form dissolution pores, resulting in pore throat enlargement and better physical properties. When salinity is low, the content of carbonate minerals increases with the increase in salinity. However, in the case of high salinity, the content of carbonate minerals gradually decreases, but that of sulfate and gypsum increases with the increase in salinity. The texture is conducive to the development of microcracks. With the increase in salinity, the number of textures first increases and then decreases. When the content is 15 ‰−30‰, there are most abundant textures, making it most likely to form microcracks. The results of this study play an important role in promoting the study of shale in the continental lacustrine basin.

KEYWORDS

shale, saline sedimentary environment, pore throat, micropore, microcrack

1 Introduction

The microscopic pore structure characteristic of the shale matrix plays an important role in the occurrence, storage, and migration of shale gas (Wu et al., 2011; Liang et al., 2014; Wu et al., 2019). The pore structure is one of the key parameters to determine the quality of shale reservoirs and evaluate the potential of shale gas resources. The pore volume and connectivity have a great influence on the occurrence and migration of shale reservoirs. The distribution and structural characteristics of shale matrix pores play an

important role in shale gas reservoirs (Chen et al., 2017; Zhao et al., 2017; Li et al., 2018). Therefore, the characteristics and reservoir performance have become important indicators for the exploration and development of shale reservoirs (Zhou and Kang., 2016; Chen et al., 2018; Gu et al., 2018; Zeng et al., 2019).

The formation and development of shale reservoir pores are not only controlled and affected by a single element, but also influenced by the combination of rock structure, sedimentary structure, matrix structure, total organic carbon, organic matter type, basin hydrothermal upwelling, thermal evolution degree, tectonic thermal events, sedimentary environment and rate, tectonic plate evolution, and fluid and hydrological conditions (Cao et al., 2018; Cavelan et al., 2019; Zhang et al., 2019; Pan et al., 2020).

Compared to conventional reservoirs, shale reservoirs are rich in organic matter, and their abundance, type, and maturity restrict the storage space of shale by controlling the development of organic pores (Clarkson et al., 2012; Curtis et al., 2012; Mastalerz et al., 2012). The mineral composition also has an important influence on the pore structure of shale. The influence of quartz, feldspar, carbonate, and other clay minerals on the pore structure has been greatly studied before (Liu and peng, 2017; Wei et al., 2018; Wei et al., 2019). The influence factors of pore structure in shale reservoirs are not single, and the shale experiences different sedimentary environments and structural backgrounds in different regions, leading the study of the influence factors of pore structure to be more complicated (Curtis., 2002; Jarvie et al., 2007; Chao et al., 2017; Zeng et al., 2021). The degree of salinity of inland lacustrine basin will affect the abundance, mineral composition, and diagenesis evolution of shale organic matter, so it must have an important impact on the

pore structure of shale. However, scholars have not done in-depth research on this.

Based on the influence of different salty environments on shale mineral composition, lithological combination, and grain layer, this study analyzes the influence of different salty environments on the shale pore structure and plays an important role in promoting the its influence factors.

2 Geological setting

The Jiyang Depression belongs to the secondary structural unit of the Bohai Bay Basin and is a fault depression superimposed basin formed in the period of Mesozoic and Cenozoic. The Dongying Sag is located in the south of the Jiyang Depression. The deep fault in the north contacts the Chenjiazhuang Uplift and Binxian Uplift. It extends to Southwest Shandong Uplift in the south, Qingtuozi Uplift in the East, and Linfanjia low Uplift in the west. It is a Meso-Cenozoic dustpan fault depression with a fault in the north and a super in the South (Figure 1). During the sedimentary period of the Shahejie Formation in the Paleogene, the basin entered the peak period of fault depression, and four sets of effective source rocks were developed: the upper Es_4, the lower Es_3, the central Es_3, and Es_1 (Song et al., 2004). Among them, the mud shale of the upper Es_4 deposited in salt semi-saltwater environment is mainly distributed in the Dongying and Zhanhua Sag, and Dongying Sag is the most developed. Mud shale in the lower Es_3 deposited in a brackish water environment is distributed throughout the region (Li., 2003).

3 Data and methods

3.1 Data

The data used in this research were provided by the Research Institute of Exploration and Development, Sinopec Shengli Oilfield Company, which includes core, logging, element, organic geochemistry, thin section, nuclear magnetic resonance, rock mechanical parameters.

3.2 Paleosalinity restoration method

Because shale inclusions are small and difficult to identify, and considering data factors, the Couth method and Sr/Ba ratio are used to restore paleosalinity.

Couth method: the amount of boron absorbed and fixed by clay minerals is related to the concentration of boron in solution, which is a linear function of salinity. By combining these two relations, Couth obtained a more reasonable paleosalinity

FIGURE 1
Regional geological survey of the Jiyang Depression.

FIGURE 2
Correlation diagram between Sr/Ba values and paleosalinity in the study area.
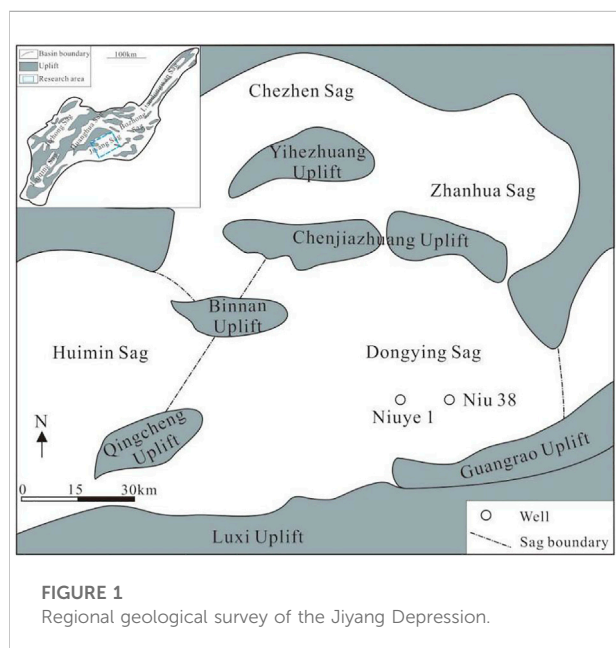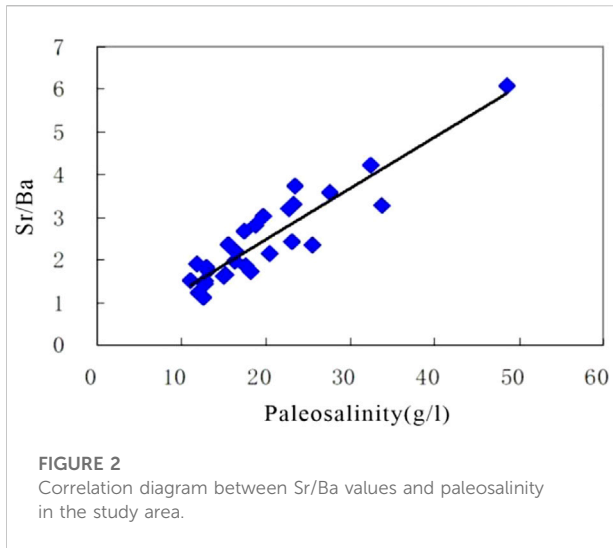
calculation formula based on the Freundlich absorption equation and the previous research results:

$$lg B_k = 1.28 lg S_p + 0.11 \qquad (1)$$

In the previous formula, B_k is the correct boron content for kaolinite (10^{-6}) and S_P paleosalinity is used for this purpose (‰). The boron content correction in this formula is based on the ratio relationship between the total amount of sample absorbed boron and the relative content of various clay minerals, which has a wide application range of salinity (1‰–35‰).

The strontium barium method is one of the common methods to restore paleosalinity. The chemical properties of strontium and barium are similar, but they are separated in different sedimentary environments due to the differences in geochemical behavior. Therefore, the strontium and barium ratio (Sr/Ba) can be used as a marker of paleosalinity (Landergren and Carvajal., 1969). Due to the strong migration capacity of strontium, when freshwater and seawater are mixed, Ba^{2+} in freshwater and SO_4^{2-} in seawater firstly combine to form $BaSO_4$ precipitation. However, Sr^{2+} can migrate to the open sea and precipitate by biological means. Therefore, the Sr/Ba value is gradually increased as it is far away from the coast, which can qualitatively reflect the paleosalinity according to its ratio. According to the statistics of 13 seabed samples in China, generally speaking, the Sr/Ba value in freshwater sediment is less than 1, whereas the Sr/Ba value in marine sediment is greater than 1, and the Sr/Ba value of 1.0–0.6 is a brackish water environment (Zhou et al., 1984; Yan, 2013).

Studying the correlation between the Sr/Ba value and paleosalinity in the study area showed a positive correlation between the two. The study data showed that, with the increase in

FIGURE 3
Vertical variation of paleosalinity in the Dongying Sag.
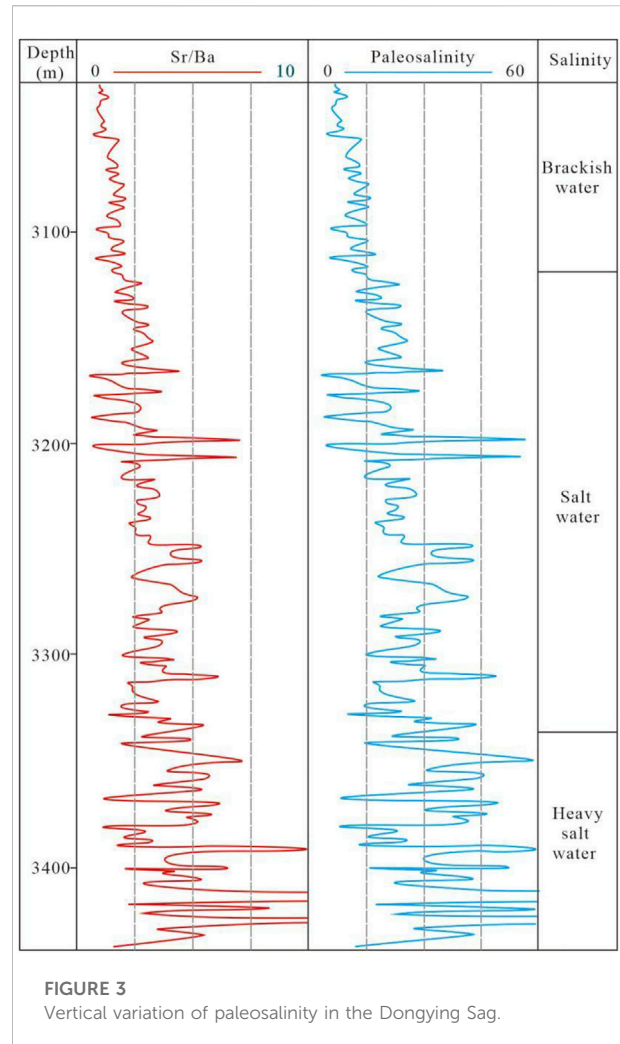
the Sr/Ba value, paleosalinity increased accordingly, and the correlation coefficient reached 0.84 (Figure 2).

4 Results

4.1 Salinity stage division

According to the research needs, this study adopts the Huang Difan (1995) paleosalinity division scheme, dividing the salinity into five intervals: freshwater stage (0.5‰–1‰), brackish water stage (1‰–5‰), brackish water stage (5‰–15‰), mixohaline water stage (15‰–30‰), and high saline stage (>30‰).

The sedimentary period of the Shahejie Formation in Dongying Sag was generally affected by the saltwater environment. Vertically, the lower segment is mainly in the saltwater high saltwater evolution stage, and the upper segment is basically in the brackish water saltwater evolution

FIGURE 4
Characteristics of salt minerals in the Dongying Sag. **(Ai)**. Swallow-tailed. **(Aii)** Creep state. **(Aiii)** Branch. **(Bi)** Lamellar. **(Bii)** Lentoid. **(Biii)** Massive. **(Biv)** Dolomite.
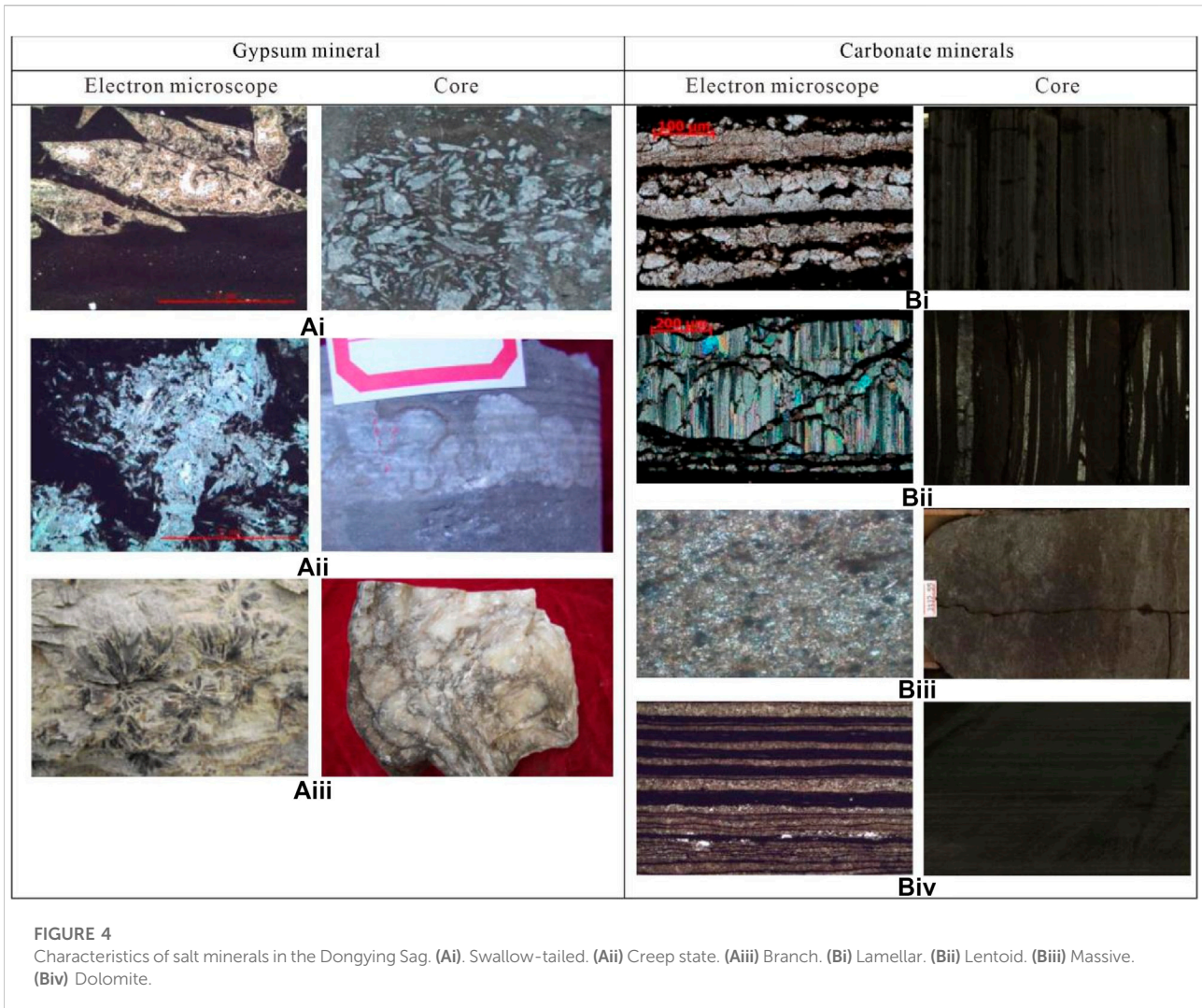
stage (Figure 3). On the plane, most areas of the Dongying Sag are of a saline water environment. Only the edge of the sag is affected by the desalination of foreign freshwater, and the paleosalinity decreases sharply.

4.2 Shale sedimentary characteristics

4.2.1 Main salt minerals and their characteristics

There are three main types of salt minerals in the study area: carbonate, sulfate, and halides. Carbonate deposition mainly includes calcite and dolomite. Sulfate deposition mainly includes gypsum and anhydrite. Halide deposition is mainly stone salt.

The microstructure of carbonate and sulfate minerals is quite complex. The main microstructure of sulfate mainly includes swallow-tailed (Figure 4Ai), creep (Figures 4Aii), and branch (Figures 4Aiii). The microstructure of carbonate

minerals mainly includes layer (Figures 4Bi), lens (Figures 4Bii), block (Figures 4Biii), and dolomite (Figures 4iv).

4.2.2 Main shale types and characteristics

From the perspective of the degree of organic matter abundance and sedimentary lithology characteristics of lithology, the research area mainly develops organic matter layer limestone, rich organic matter layer limestone, rich organic matter layer, rich organic matter, and rich organic matter grain. The various lithological microscopic characteristics are as follows:

4.2.2.1 Argillaceous limestone containing organic matter grain layer

The color is light, characterized by the horizontal distribution of light and dark layers (Figure 5A), and the light layer has low recrystallization. The light layer is calcite
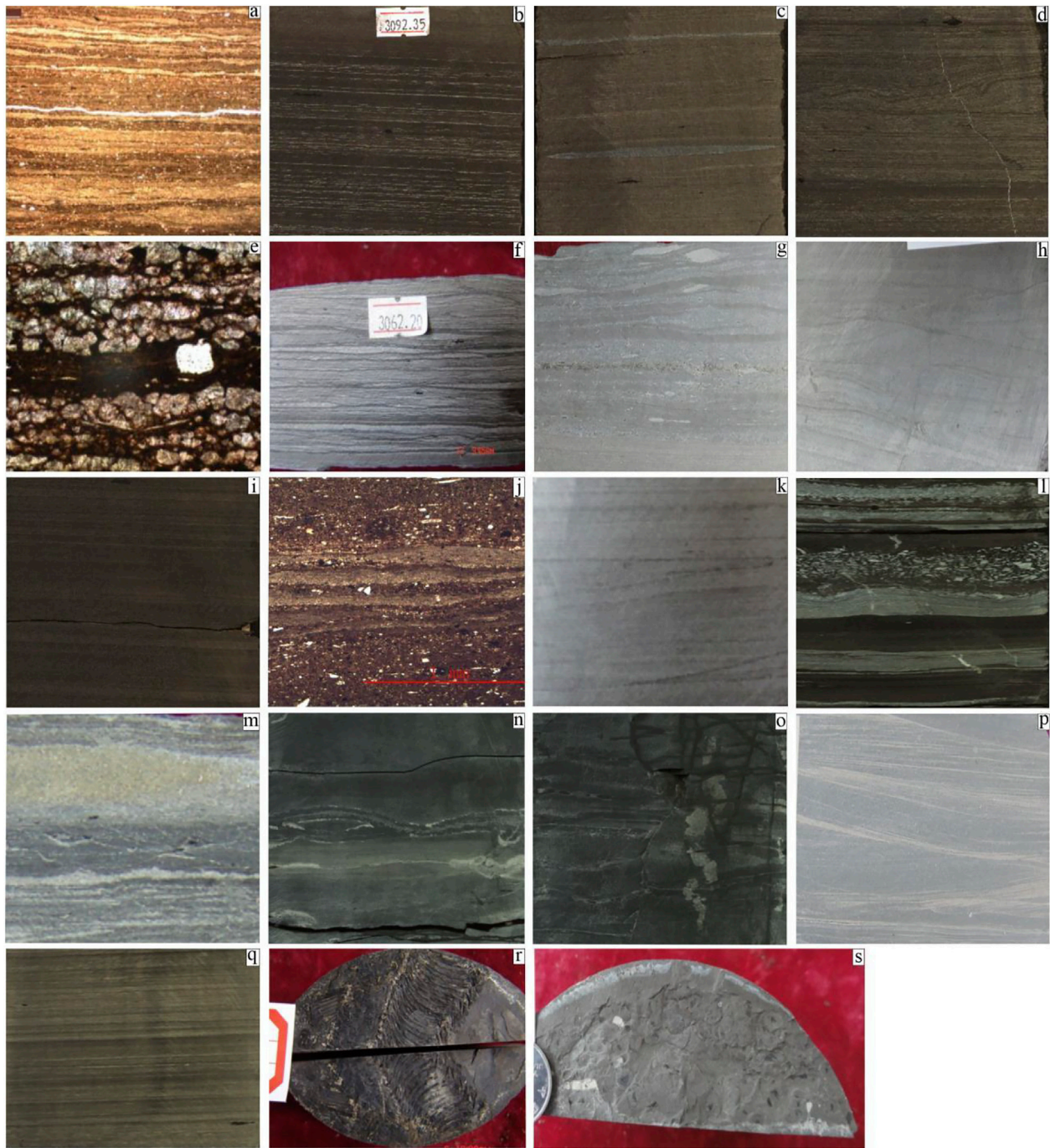
FIGURE 5
Main shale types and characteristics in the core. **(A−D)** Well Luo 69, 3,070.6−3,127.1 m, contains organic grain layered argillaceous limestone. **(E−H)** Well Luo 69, 3,040−3,070.6 m, contains organic grain layered argillaceous limestone. **(I−K)** Well Luo 69, 3,015−3,040.55 m, rich organic grain layered clay limestone. **(L,M)** Well Niuye 1, 3,490−3,500 m. **(N−P)** Well Niuye 1, 3,070−3,076.5 m, contains organic massive gray mudstone. **(Q−S)** Well Niuye 1, 3,402.7−3,452 m, rich organic grain layered gray mudstone.

(Figure 5B), and the dark layer is clay ore, occasionally silty interlayer (Figure 5C), staggered layer (Figure 5D), and rare microfossils. The main organic carbon content is mostly less than 2%. Most components are mainly carbonate rock, followed by quartz plus feldspar and clay minerals.
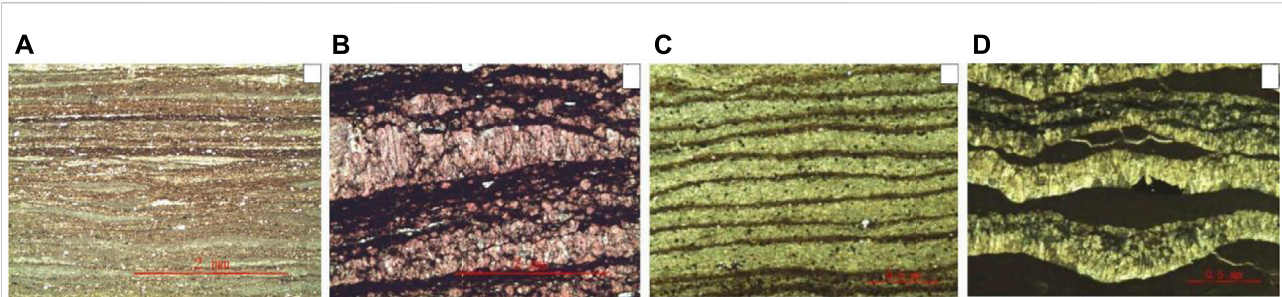
FIGURE 6
Type and characteristics of shale texture. **(A)** Sedimentary formation of grain layer. **(B)** The grain layer **(C)**, which is inherited from deposition and mainly formed by diagenesis. Granular calcite and mud layer interlayer. **(D)** Fragmented sedimentary layers are visible in the columnar calcite stripes.
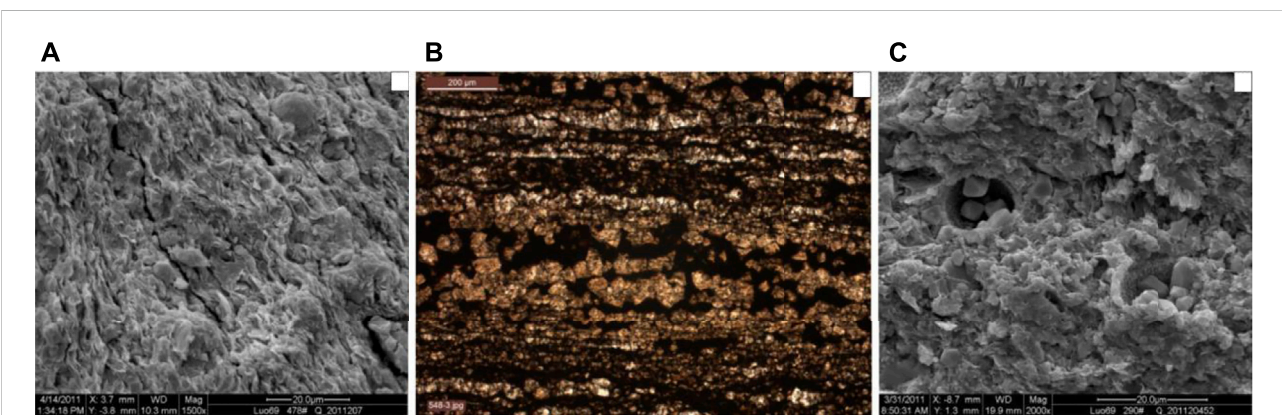
FIGURE 7
Type and characteristics of shale pore throat. **(A)** Well Luo 69, 3,039.60 m, sheet micropore development; see strawberry pyrite. **(B)** Well Luo 69, 3,055.60 m. **(C)** Well Luo 69, 2,992.60 m, Micropores were developed in calcite, clay and pyrite crystals. Asphaltene was found between calcite crystals.

4.2.2.2 Rich in organic grain layered argillaceous limestone

The color is light, characterized by a light and dark horizontal grain layer (Figure 5E), and the light color layer has a high degree of recrystallization. The light color layer is calcite, and the dark layer is clay ore (Figure 5F), with occasional lens sand strip (Figure 5G), staggered bedding, and microfossils (Figure 5H). The main organic carbon content is more than 2%. Most components are mainly carbonate rock, followed by quartz plus feldspar and clay minerals.

4.2.2.3 Organic matter-rich layered gray mudstone

The color is darker, characterized by a thin reciprocal layer distribution of the light and dark phase (Figure 5I), and the crystallization degree of the light color layer is low. The light layer is calcite, and the dark layer is clay ore (Figure 5J), occasionally lenticular sand strip, staggered layer (Figure 5K); a large number of Ostracoda fossils can be seen. The vast

majority of the organic carbon content is more than 2%. The components are mainly carbonate rock, high clay mineral content, followed by quartz plus feldspar.

4.2.2.4 Compound mudstone containing organic matter layer

The color is light, characterized by a thin reciprocal layer distribution between light and dark (Figure 5L). The dark layer is gray matter mudstone, and the light color layer is plaster rock or argillaceous paste rock; a large number of pyrite can be seen (Figure 5M). The organic carbon content is very little, and the vast majority are less than 2%. On the components, there are carbonate rock, gypsum, clay minerals, and quartz plus feldspar, of which the carbonate rock content is slightly higher, followed by gypsum.

4.2.2.5 Organic matter massive gray mudstone phase

The color of this lithology is relatively light, mainly gray–blue gray. It is dominated by massive structures with visible wave

FIGURE 8
Microscopic characteristics of microcracks. **(A)** Along the layer of microcracks, bright yellow fluorescence. **(B)** Overpressure crack is filled with bright crystal calcite. **(C)** Calcite half-filling, high Angle inclined intersection joint contains oil. **(E)** Gray mudstone, unfilled with microcracks, produces green light.
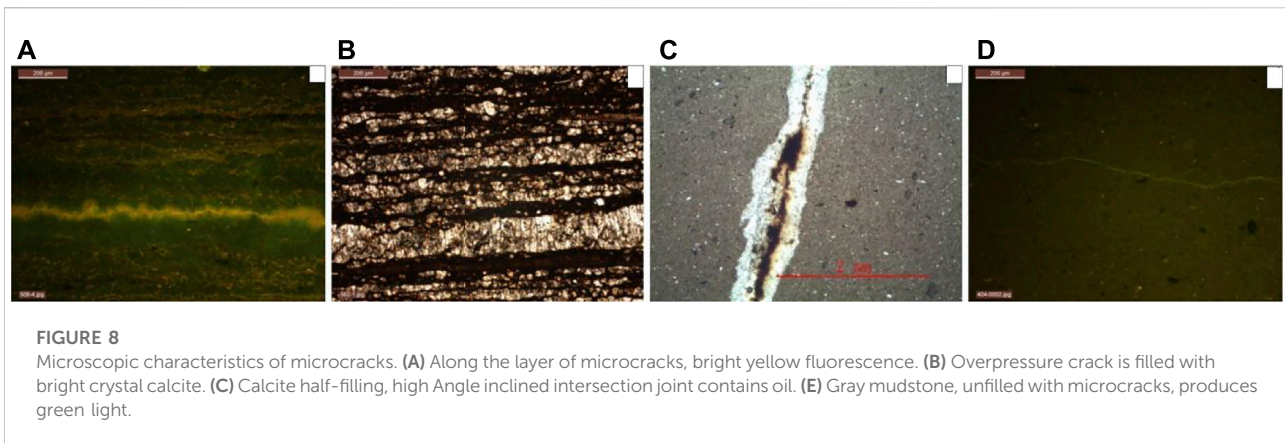
bedding (Figure 5N), sandy masses (Figure 5O), and staggered bedding (Figure 5P). The organic carbon content is very little; most are less than 2%, the components with carbonate rock, clay minerals, and quartz plus feldspar, of which the content of clay minerals is slightly higher. The color mutation on the core and the organic matter content from high to low values are considered event deposition.

4.2.2.6 Rich in organic grain layered limestone mudstone

The color is darker, characterized by the horizontal distribution of the layer (Figure 5Q). The light color grain layer is calcite, recrystallization, or a mixed layer of clay minerals and cryptocrystalline calcite, and the dark color grain layer is organic matter and clay. Fossil fish species (Figure 5R) and ostracodes (Figure 5S) were visible in the core observation. Organic carbon content is very high, and most are more than 2%. There are carbonate rock, clay minerals, quartz plus feldspar, and pyrite on the components, of which the total amount of carbonate is slightly higher.

4.2.3 Type and characteristics of the shale layer

From the perspective of the causes of grain layer, the grain layers mostly formed by deposition are fine and dense and often appear as layer even, which is manifested as the combination characteristics of mud grain layer plus gray grain layer, mud grain layer plus organic grain layer, and plaster grain layer plus organic grain layer. This kind of grain layer can be understood as the seasonal pattern layer, resulting from a combination of climate, biological, and land-based material input and preservation conditions (Figure 6A).

The grain layers mainly formed by deposition and diagenesis have obvious differences. The gray matter grain layer is formed by bright crystal calcite, the thickness can reach more than 1 cm, and some cores are clearly visible. This kind of layer is a common transition state with the upper kind of layer, so it is speculated that it results from inheritance deposition and diagenetic

transformation. The common bright calcite stripes arranged along the layers can be classified into two categories: granular calcite stripes and columnar calcite stripes. Granular calcite stripe is a sedimentary-diagenesis cause, mainly caused by recrystallization of sedimentary gray grain layer. In contrast, column calcite stripe is the cause of over-compression fracture filling of hydrocarbon source rock (Figure 6B).

Interbedded granulated calcite and argillaceous laminae are seasonal sedimentary laminae. The thickness of each layer is uniform and thin (generally between 0.10 and 0.30 mm). The particle size varies from fine to coarse and contains deposited impurities (the color is yellow under the monopolarizer). The residual early fine-grained structures in the laminae indicate recrystallization or multi-stage recrystallization diagenesis, which is controlled by both sedimentary and diagenetic factors (Figure 6C).

When mineralized water rich in calcium carbonate is filled in the shale, it will precipitate, crystallize, grow and fracture the shale, so fragmented sedimentary lamina can be seen in the columnar calcite streaks. The distribution of calcite laminae has poor interlaminae with mud laminae, but many parallel laminae occur, and can coexist with granular calcite laminae. The width range of calcite lamina is large, which can be less than 0.05 mm or more than 10 mm. Under the action of longitudinal tension and transverse pressure, calcite was vertically bedded into columnar growth, belonging to the single controlled diagenetic origin (Figure 6D).

4.3 Type and characteristics of shale pore throat

Fractures are a key factor in unconventional reservoir development (Zhao et al., 2021). By analyzing the characteristics of shale storage, it is believed that the shale storage space mainly has micropores (organic pores, intercrystal pores, and intergrain pores) and microcracks
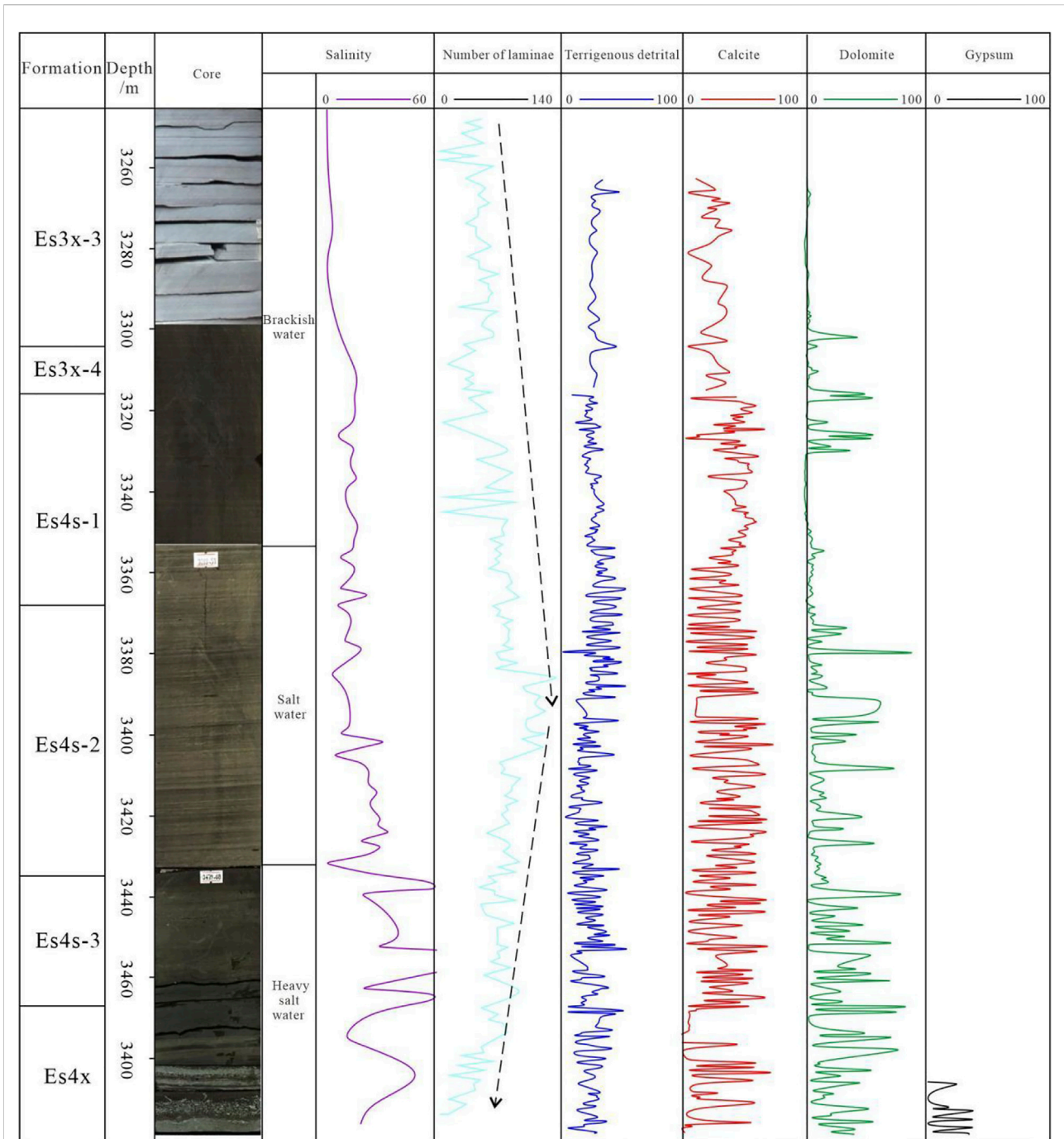
FIGURE 9
Relationship between the saline stage and lithological sedimentation and texture (Well Niu 38 and Well Niuye 1)

(along-layer cracks, high-pressure cracks, structural cracks, and mineral shrinkage joints). The type and development degree of these joints are often controlled by salinity.

4.3.1 Intercrystalline micropores of clay pore

Clay minerals are mainly illite/smectite and illite, with strong orientation, so the intercrystalline micropores are mainly sheet-shaped (Figure 7A), and the size is mostly below 5 m.

FIGURE 10
Plot of carbonate mineral structure and paleosalinity.
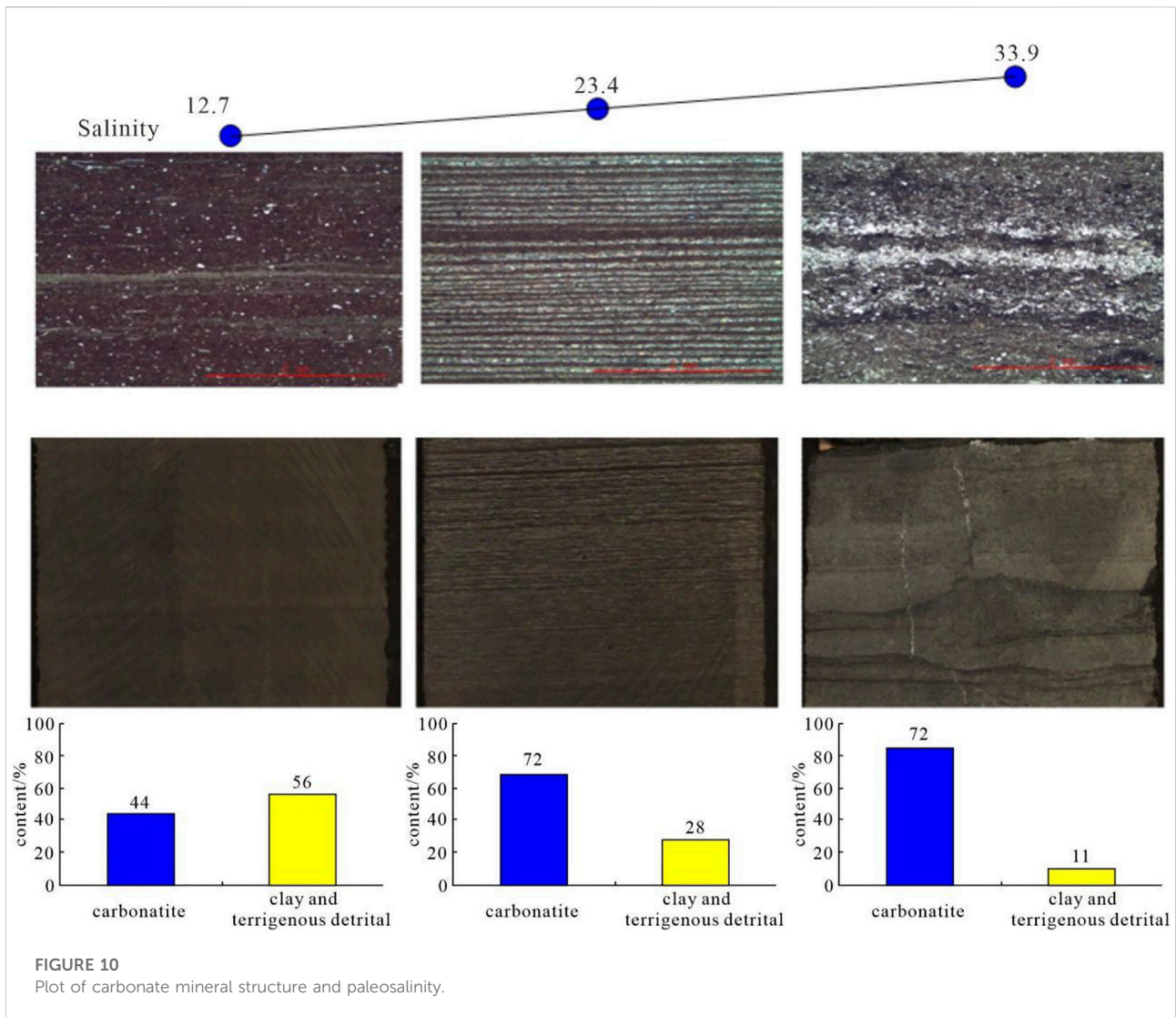
4.3.2 Calcite intercrystal pore

Calcite is the main mineral in this layer, the main hidden crystal structure, and part of the micro-crystal structure; it often constitutes the gray matter layer or is mixed with mud minerals output. Under the polarizing microscope, the gray crystal contains black asphaltene umen (Figure 7B), which is an important pore type, up to 50 µm; the crystal and clay ore micropores overlap (Figure 7C), so they are mostly below 5 m.

4.3.3 Pyrite intercrystalline micropores

Pyrite is a self-occurring mineral in a reducing environment. It is often dispersed as a strawberry aggregate, and its crystal shape is intact, so micropores below micrometers are often developed (Figure 7C).

4.3.4 Micropores between sand plasmids

Land-based sand is often dispersed in the mud or produced as strips. Electron microscope observation of the sand strip shows the interparticle micropores.

Pore type is closely related to rock composition, high calcite content easily forms granular intercrystalline pores, and high clay minerals mainly form sheet micropores. In addition, the pore type is also closely related to the evolution of hydrocarbon source rock. Gray matter source rock rich in organic matter easily forms overpressure cracks in the process of hydrocarbon pressurization, which is the most favorable area for forming calcite intercrystalline pores.

4.3.5 Cracks

According to the causes, it can be divided into diagenesis microcracks and structural microcracks. The former mainly

FIGURE 11
Plot of salinity and layer structure.
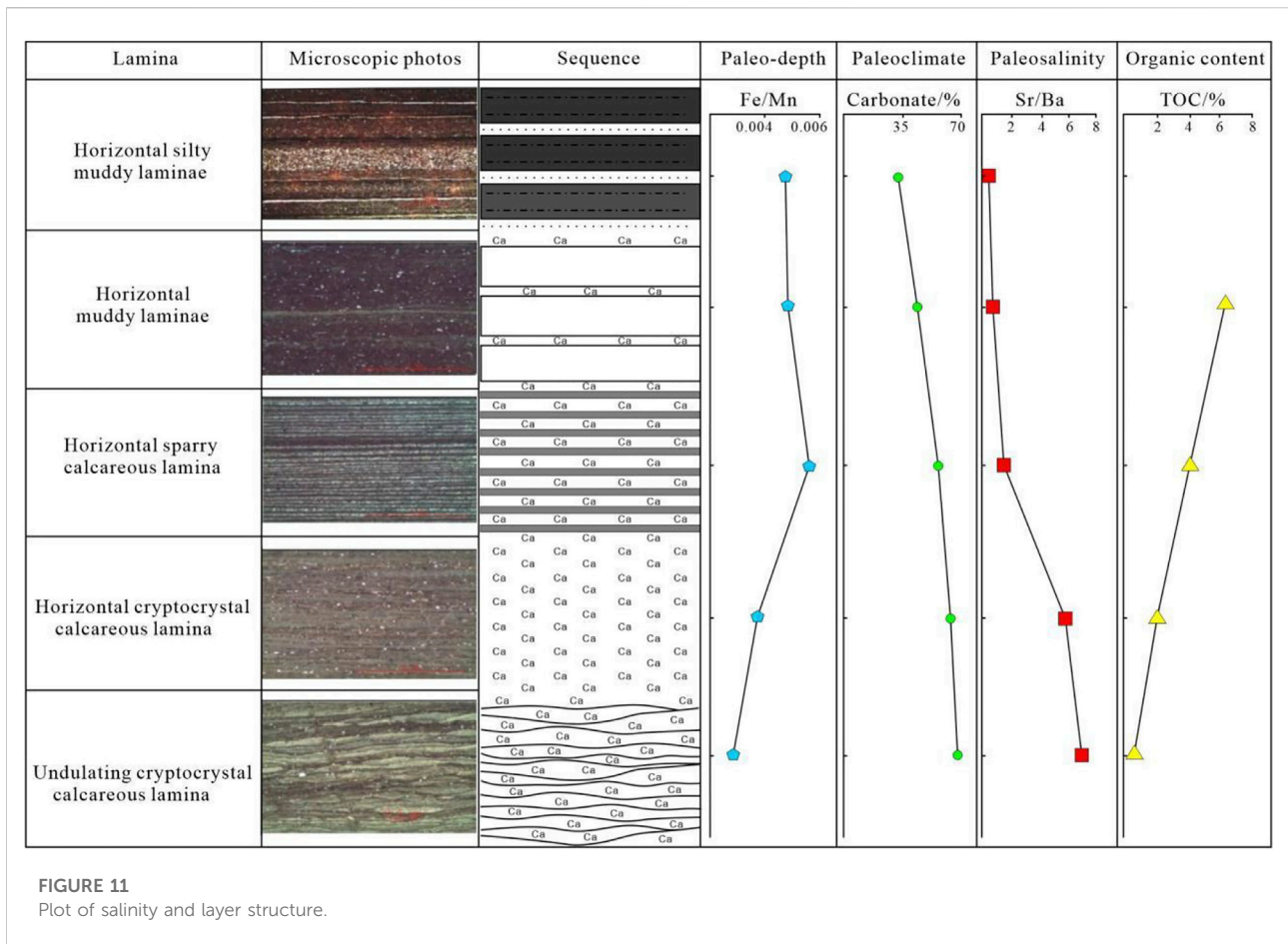
includes interlayer microcracks and overpressure microcracks (filled by bright crystal calcite or dolomite); the latter is mainly inclined cracks according to the production and near vertical level cracks, which can be divided into filling, semi-filling, and unfilled according to the filling degree. In general, the crack type is mainly identified by the smooth layer microcracks, followed by the structural joint.

4.3.5.1 Interlayer microcracks

It often develops between different components (Figure 8A), with a narrow width, all below 0.02 mm. However, its significance lies in the development of potential microcracks and being easy to continue along the layer.

4.3.5.2 Ultra-pressure microcracks

In the process of hydrocarbon pressurization evolution, hydrocarbon source rocks have a large number of drainage and various cations, so they often cause mineral dissolution and reprecipitation. The recrystallized calcite crystals are filled in the smooth crack produced in the pressurization process (Figure 8B), and the recrystallized crystals often develop intercrystalline pores.

4.3.5.3 Structure crack

The surface of structural fractures in the core is relatively flat, which often causes dislocation of the grain plane. These cracks are often filled with calcite, but residual pores can be seen under the mirror and filled with black bitumen umen (Figure 8C), which is evidence of oil and gas transport. In addition, irregular unfilled microcracks were found under the polarized microscope (Figure 8D).

5 Discussion

5.1 Minerals and lithological differences in different saline stages

There is a good correspondence between paleosalinity and salt minerals, which has increased significantly with the increase in paleosalinity. Before the high saline stage, carbonate minerals increased significantly with the increase in paleosalinity. However, when the paleosalinity increased to a certain extent, carbonate minerals gradually decreased, sulfate minerals and halide minerals began to

FIGURE 12
Plot of pore types in different saline stages.
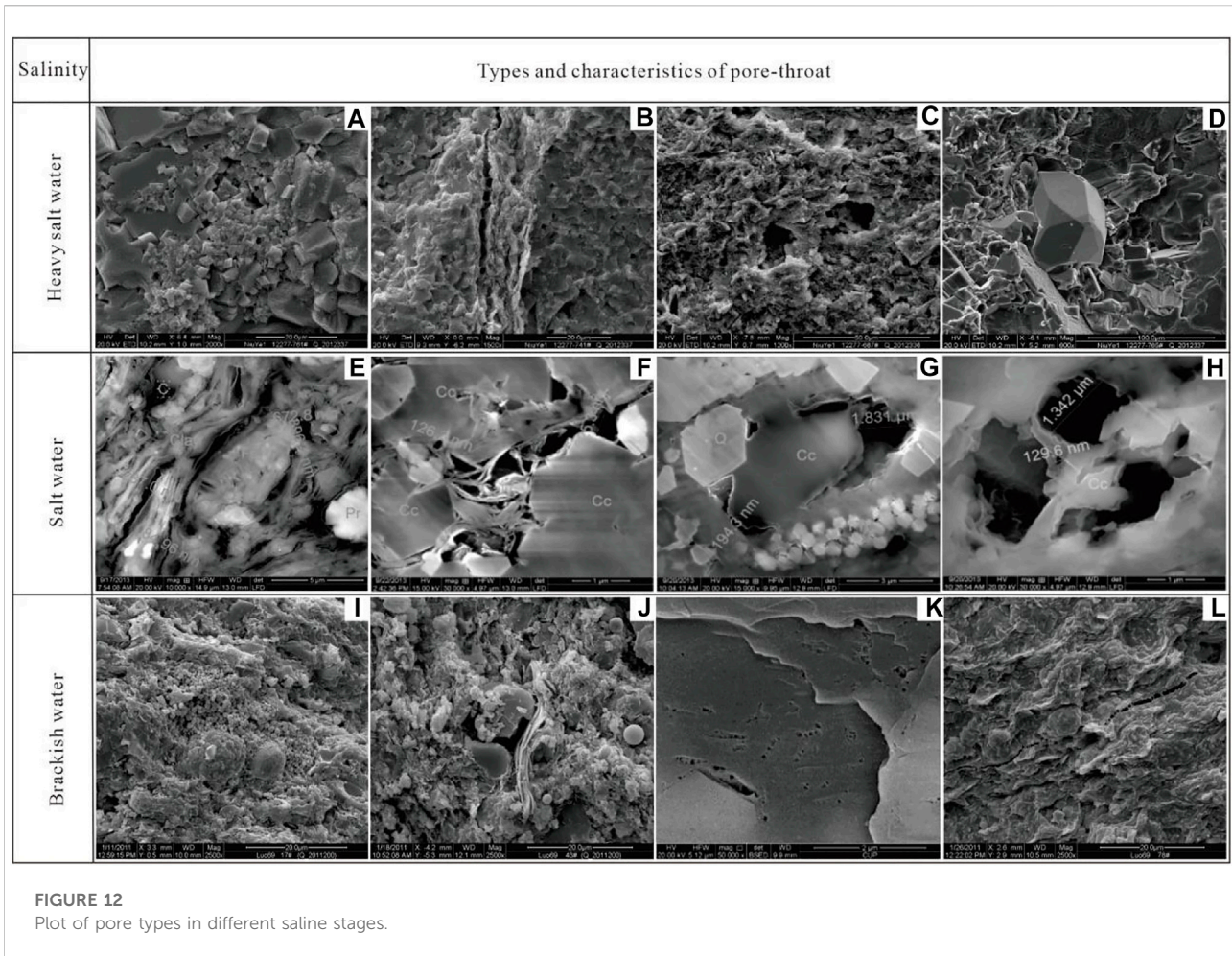
TABLE 1 Statistical table of crack influencing factors.

Bedding type	Lamina		Stratiform	Bulk
	Straightness	**Microwave**		
Degree of microcrack development	++++	+++	++	+
Main types of microcracks	Along crack (page crack)	Along crack (page crack)	Along the crack	Astatic
Type of rock composition	Mud stone	Marlite	Grey rock, mudstone	Muddy sandstone
Degree of microcrack development	++++	++++	++	+

develop, and the content increased with the increase in salinity.

Salinity controls the evolution sequence of lithology. When the paleosalinity was in the high saline stage, the dolomite content of the three lower subsections changed a little, and the upper subsection of sand increased significantly. However, gypsum, anhydrite, rock salt, and barite only began to appear from the upper subsection of sand (pure lower subsection). The lithology in the high saline stage, brackish stage and brackish water-brackish stage is mainly composed of paste - mudstone assemblages, carbonate rocks - laminated mudstone assemblages and layered mudstone - massive mudstone assemblages, respectively. When the salinity ranges from 15‰ to 30‰, the carbonate stratum is the most developed (Figure 9).

5.2 Relationship between saline environment and shale microstructure

The degree of grain layer development is closely related to the paleosalinity. Through the statistical estimation of the pattern value in Well Luo 69 in the Bohai south area and Well Niuye 1 in the Dongying Depression and the comparative analysis of the relationship between the number of layers and the paleosalinity, it is found that, with the increase in paleosalinity and when it reaches a certain degree, the number of layers shows a trend of decreasing. When the paleosalinity is in the range of 15 ‰–30‰, the carbonate pattern layer is the most developed (Figure 9).

The microstructure of salt minerals is also closely related to their salinity. Taking the interlayer structure of carbonate minerals as an example, the study area of layered carbonate minerals appeared mostly in carbonate and mudstone (or organic matter). The results show that, with the gradual increase in paleosalinity, the content of carbonate rock increases. The carbonate content is reduced when the salinity is low. The content of clay and land-based debris is too low for developing layer deposition (Figure 10).

The internal structure of the chemical origin of stratified lithology is obviously controlled by the paleosalinity. With the evolution of paleosalinity from high to low, the microstructure of the grain layer is characterized by the change characteristics of the undulating cryptocrystal calcareous lamina, horizontal sparry calcareous lamina, horizontal muddy laminae and horizontal silty muddy laminae (Figure 11). This evolution may be related to the chemical origin of the carbonate rocks in this region.] The development of "biogenic carbonate plus mudstone/organic matter" and "muddy silt plus clay/organic matter" layer is obviously controlled by biological development and material source (Figure 12).

5.3 The relationship between saline environment and shale pore throat

The study of the relationship between salinity and lithology and storage showed that different lithological combinations developed in different salination stages, and different lithological combinations developed in different lithological combinations (Figure 12).

In the high saline stage, there are mainly paste mudstone and dolomite, corresponding to the main development of hydrgypsum intercrystalline pores (Figure 12A), dolomite intercrystalline pores (Figure 12B) and some dissolved pores (Figures 12C,D). Both gypsum and anhydrite are sulfate minerals (the gypsum chemical formula is $CaSO_4 \bullet 2H_2O$, and the anhydrite chemical formula is $CaSO_4$), and Has a certain degree of plasticity. Usually, gypsum can be formed in a natural state, losing water at 80°C–90°C, converting into hydraster, and forming substable plaster at 100°C, stable plaster at 150°C, and stable plaster at 193°C. Taking Bonnan depression as an example, according to the ground temperature gradient of 3.5°C/

100 m, the ground temperature can reach 123°C at 3,500 m. At this time, the gypsum has been fully transformed into anhydrite, and the ground temperature at 4,500 m is about 158°C. At this time, the gypsum has been fully transformed into anhydrite. Thus, the salt layer developed in the deep layer of Bonan depression is basically anhydrite. On the one hand, the formation of anhydrite in the Bonan depression suppresses the compaction effect, enabling the preservation of the native pores of the reservoir. On the other hand, the existence of the paste salt layer strengthens the fluid-rock action, especially the dissolution effect, making water discharged by the gypsum transformation, and dissolving organic acids, thus further dissolving rock minerals and forming secondary pore zones.

In the saltwater stage, there are mainly developed layered clay limestone/gray clay limestone and layered limestone, and corresponding to some intergranular pores (Figures 12E,F), dissolution pores(Figures 12G,H) and interlayer cracks.

The brackish water-brackish water stage mainly develops layers/massive gray mudstones/mudstones, corresponding to the main developing intergranular pores (Figures 12I,J), biological pores (Figure 12G,K) and microcracks (Figure 12I).

From the perspective of lithology, different layer types and rock compositions have a great impact on the development degree of microcracks, especially along the substrata. Statistical findings (Table 1): the smooth layer microcracks of plain layered mudstone and mudstone are the most developed, and the second is microcorrugated layered marl, layered mudstone, and limestone, and the worst is block. The contact area between straight layers is smaller than that of corrugated layers, the binding force between layers is weak, and it is relatively easy to crack into cracks under overpressure.

6 Conclusion

This study aims to clarify the effect of the continental lacustrine basin on shale pore throat. By studying the shale of the Shahejie Formation in the Jiyang Depression, China, conclusions are drawn as follows.

1. Carbonate minerals are the most abundant minerals in shale. In the case of low salinity, the content of carbonate minerals increases with the increase in salinity. In the case of high salinity, the content of carbonate minerals gradually decreases while that of sulfate and gypsum increases with the increase in salinity. The assemblage of gypsum stone-argillite, carbonate rock-laminated argillite, and laminated calcareous mudstone-massive are developed, respectively, in the high saline, saltwater, and brackish stages. The carbonate laminae are most developed when the salinity ranges from 15‰ to 30‰.

2. The texture is conducive to the development of microcracks. With the increase in salinity, the number of textures first

increases and then decreases. When the content is 15 ‰–30‰, there are most abundant textures, making it most likely to form microcracks.

3. The lithological assemblage controls the original pore throat type of shale. The carbonate minerals are prone to dissolution, which enlarges the pore throat. Microcracks are very likely to emerge on the grain layer in the later stage. The more the grain layers, the more the microcracks. Carbonate minerals and grain layers are the main factors to improve the structure of shale pores.

Data availability statement

The original contributions presented in the study are included in the article/Supplementary Material. Further inquiries can be directed to the corresponding author.

Author contributions

ZZ is responsible for writing the entire article. SW and MH are responsible for experiments and data. YF is responsible for writing ideas and revising articles.

Conflict of interest

Author SW was employed by Sinopec Shengli Oilfield Company. Author MH was employed by CNOOC Research Institute Ltd. Author YF was employed by CNPC Xibu Drilling Engineering Company Limited.

The remaining authors declare that the research was conducted in the absence of any commercial or financial relationships that could be construed as a potential conflict of interest.

Publisher's note

All claims expressed in this article are solely those of the authors and do not necessarily represent those of their affiliated organizations or those of the publisher, the editors, and the reviewers. Any product that may be evaluated in this article, or claim that may be made by its manufacturer, is not guaranteed or endorsed by the publisher.

References

Cao, T., Liu, G., Cao, Q., and DengM (2018). Influence of maceral composition on organic pore development in shale: A case study of transitional longtan formation shale in eastern sichuan basin. *Oil Gas Geol.* 39 (1), 40–53. doi:10.11743/ogg20180105

Cavelan, A., Boussafir, M., Milbeau, C. L., Rozenbaum, O., and Laggoun-Defarge, F. (2019). Effect of organic matter composition on source rock porosity during confined anhydrous thermal maturation: Example of Kimmeridge-clay mudstones. *Int. J. Coal Geol.* 212, 103236. doi:10.1016/j.coal.2019.103236

Chao, P., Pan, J., and Wan, X. (2017). Effect of clay minerals of coal-bearing shale on pore structure and methane adsorption property in Yuzhou coalfield. *China coal.* 43 (06), 46–52.

Chen, K. L., Zhang, T. S., and Liang, X. (2018). Analysis of shale lithofacies and sedimentary environment on wufeng formation-lower longmaxi Formation in dianqianbei depression. *Acta Sedimentol. Sin.* 36 (04), 743–755.

Chen, L., Jiang, Z., Liu, K., Tan, J., Gao, F., and Wang, P. (2017). Pore structure characterization for organic-rich lower silurian shale in the upper Yangtze platform, south China: A possible mechanism for pore development. *J. Nat. Gas Sci. Eng.* 46, 1–15. doi:10.1016/j.jngse.2017.07.009

Clarkson, C. R., Jensen, J. L., Pedersen, P. K., and Freeman, M. (2012). Innovative methods for flow-unit and pore-structure analyses in a tight siltstone and shale gas reservoir. *Am. Assoc. Pet. Geol. Bull.* 96 (2), 355–374. doi:10.1306/05181110171

Curtis, J. B. (2002). Fractured shale-gas systems. *AAPG Bull.* 86 (11), 1921–1938.

Curtis, M. E., Cardott, B. J., Sondergeld, C. H., and Rai, C. S. (2012). Development of organic porosity in the Woodford Shale with increasing thermal maturity. *Int. J. Coal Geol.* 103, 26–31. doi:10.1016/j.coal.2012.08.004

Gu, Y., Ding, W., Yin, M., Jiao, B., Shi, S., Li, A., et al. (2018). Nanoscale pore characteristics and fractal characteristics of organic-rich shale: An example from the lower Cambrian Niutitang Formation in the Fenggang block in northern Guizhou Province, South China. *Energy Explor. Exploitation* 37 (1), 273–295. doi:10.1177/0144598718790320

Jarvie, D. M., Hill, R. J., Ruble, T. E., and Pollastro, R. M. (2007). Unconventional shale-gas systems: The Mississippian Barnett Shale of north-central Texas as one model for thermogenic shale-gas assessment. *Am. Assoc. Pet. Geol. Bull.* 91 (4), 475–499. doi:10.1306/12190606068

Landergren, S., and Carvajal, M. C. (1969). Geochemistry of boron, II. The relationship between boron concentration in marine clay sediments expressed as an adsorption isotherm. *Ark. Kem. Mineral. Geol.* 5, 13.

Li, A., Ding, W., Jiu, K., Wang, Z., Wang, R., and He, J. (2018). Investigation of the pore structures and fractal characteristics of marine shale reservoirs using nmr experiments and image analyses: A case study of the lower cambrian niutitang Formation in northern guizhou province, south China. *Mar. Pet. Geol.* 89, 530–540. doi:10.1016/j.marpetgeo.2017.10.019

Li, P. L. (2003). "Petroleum geology and exploration of continental fault basin," in *Hydrocarbon generation and resource evaluation of continental fault basin*. (Beijing: Petroleum Industry Press) Vol. 3, 4–8.

Liang, X., Zhang, T., and Yang, Y. (2014). Microscopic pore structure and its controlling factors of overmature shale in the Lower Cambrian Qiongzhusi Fm, northern Yunnan and Guizhou provinces of China. *Nat. Gas. Ind.* 34 (02), 18–26.

Liu, Y., and Peng, P. A. (2017). Research on the influences of different mineral compositions on the development of nanopores in shales. *J. CHINA COAL Soc.* 042 (003), 702–711.

Mastalerz, M., He, L., Melnichenko, Y. B., and Rupp, J. A. (2012). Porosity of coal and shale: Insights from gas adsorption and SANS/USANS techniques. *Energy fuels.* 26 (8), 5109–5120. doi:10.1021/ef300735t

Pan, B., Gong, C., Wang, X., Li, Y., and Iglauer, S. (2020). The interfacial properties of clay-coated quartz at reservoir conditions. *Fuel* 262, 116461. doi:10.1016/j.fuel.2019.116461

Song, G. Q., Wang, Y. S., Cheng, F. Q., Company, S. O., and SINOPEC (2004). Ascertaining secondary order sequence of Palaeogene in Jiyang depression and its petroleum geological significance. *Petroleum Geology and Recovery Efficiency* 21 (5), 1–7.

Wei, M., Zhang, L., Xiong, Y., and Peng, P. (2019). Main factors influencing the development of nanopores in over-mature, organic-rich shales. *Int. J. Coal Geol.* 212, 103233. doi:10.1016/j.coal.2019.103233

Wei, Z., Wang, Y., Wang, G., Sun, Z., and Xu, L. (2018). Pore characterization of organic-rich late permian da-long formation shale in the

sichuan basin, southwestern China. *Fuel* 211, 507–516. doi:10.1016/j.fuel.2017. 09.068

Wu, L. M., Ding, W. L., and Zhang, J. C. (2011). Fracture prediction of organic-enriched shale reservoir in lower silurian longmaxi formation of southeastern chongqing area. *J. Oil Gas Technol.* 33 (09), 43–166.

Wu, Y. Q., Tahmasebi, P., Lin, C. Y., Zahid, M. A., Dong, C., Golab, A. N., et al. (2019). A comprehensive study on geometric, topological and fractal characterizations of pore systems in low-permeability reservoirs based on SEM, MICP, NMR, and X-ray CT experiments. *Mar. Petroleum Geol.* 103, 12–28. doi:10. 1016/j.marpetgeo.2019.02.003

Yan, S. C. (2013). Paleo - salinity and paleo - environmental analysis of Carboniferous in northeast Junggar basin. *Petroleum Geol. Recovery Effic.* 20 (5), 60–63.

Zeng, F., Dong, C. M., Lin, C. Y., Wu, Y. Q., Tian, S. S., Zhang, X. G., et al. (2021). Analyzing the effects of multi-scale pore systems on reservoir properties—a case study on xihu depression, East China sea shelf basin, China. *J. Petroleum Sci. Eng.* 203, 108609. doi:10.1016/j.petrol.2021.108609

Zeng, W., Ding, W., and Zhang, J. (2019). Analyses of the characteristics and main controlling factors for the micro/nanopores in Niutitang shale from China's southeastern Chongqing and northern Guizhou regions. *Earth Sci. Front.* 26 (3), 220–235.

Zhang, J., Li, X., Xiaoyan, Z., Zhao, G., Zhou, B., Li, J., et al. (2019). Characterization of the full-sized pore structure of coal-bearing shales and its effect on shale gas content. *Energy fuels.* 33 (3), 1969–1982. doi:10.1021/acs.energyfuels.8b04135

Zhao, P., Wang, Z., Sun, Z., Cai, J., and Wang, L. (2017). Investigation on the pore structure and multifractal characteristics of tight oil reservoirs using NMR measurements: Permian Lucaogou Formation in Jimusaer Sag, Junggar Basin. *Mar. Petroleum Geol.* 86, 1067–1081. doi:10.1016/j.marpetgeo.2017. 07.011

Zhao, Z. X., He, Y. B., and Huang, X. (2021). China, Lithosphere, 3310886. doi:10.2113/ 2021/3310886Study on fracture characteristics and controlling factors of tight sandstone reservoir: A case study on the huagang Formation in the xihu depression, East China sea shelf basin, China.1

Zhou, L., and Kang, Z. (2016). Fractal characterization of pores in shales using nmr: A case study from the lower cambrian niutitang Formation in the middle Yangtze platform, southwest China. *J. Nat. Gas Sci. Eng.* 35, 860–872. doi:10.1016/j. jngse.2016.09.030

Zhou, Y. K., He, J. W., and Wang, Z. W. (1984). *Application of boron as an indicator of paleosalinity. Selected papers from conferences on Sedimentology and Organic Geochemistry*. Beijing: science press, 55–57.